IOP Publishing — Semiconductor Science and Technology
Semicond. Sci. Technol. 32 (2017) 114007 (7pp) https://doi.org/10.1088/1361-6641/aa8d08

Optical characteristics of GaAsSb alloy after rapid thermal annealing

Xian Gao[1,2], Fenghuan Zhao[1], Xuan Fang[2], Jilong Tang[2], Dan Fang[2], Dengkui Wang[2], Xiaohua Wang[2], Zhipeng Wei[2,3] and Rui Chen[1,3]

[1] Department of Electrical and Electronic Engineering, South University of Science and Technology of China, Shenzhen, Guangdong, 518055, People's Republic of China
[2] State Key Laboratory of High Power Semiconductor Laser, School of Science, Changchun University of Science and Technology, 7089 Wei-Xing Road, Changchun, 130022, People's Republic of China

E-mail: zpweicust@126.com and chen.r@sustc.edu.cn

Received 29 June 2017, revised 11 September 2017
Accepted for publication 15 September 2017
Published 13 October 2017

Abstract

GaAsSb ternary alloy is a promising material for application in infrared optoelectronic devices. In this letter, the investigation of carrier recombination in the as-grown and rapid thermal annealing (RTA) treated GaAsSb samples has been carried out. It was found that after thermal treatment the emission of the GaAsSb material was enhanced and could be maintained up to room temperature. These phenomena can be ascribed to the decrease of non-radiative combination defects in the GaAsSb sample, which implies an improved crystal quality. Moreover, the localized exciton–longitudinal optical phonon interaction is slightly increased after RTA treatment. It is suggested that the interaction depends strongly on the localized states, and the photoluminescence emission intensity can be significantly increased after suitable RTA treatment. Promoting better optical emission in GaAsSb is very useful for its practical application.

Keywords: photoluminescence, localized state, exciton, exciton–phonon interaction, rapid thermal annealing

(Some figures may appear in colour only in the online journal)

1. Introduction

Recently, GaAsSb ternary alloys with controllable antimony (Sb) content have been studied as a promising material for near or mid-infrared optoelectronic devices, especially for multi-quantum well (MQWs) lasers [1–3]. Generally speaking, the performance of the device depends strongly on the optical properties of the materials. Although the band gap of GaAsSb alloys can be easily controlled by the Sb content, their small exciton binding energy (<10 meV) and serious emission quenching at high temperature significantly influence their optical properties. In addition, the carrier localization effect caused by fluctuations of Sb content makes the situation even more complicated. As a consequence, understanding the carrier dynamics of the materials has become one of the key research topics for improving the performance of the devices. In recent years, researchers have focused on their growth technology, quantum well structure and optical properties [4–9]. Some researchers have investigated the effect of thermal annealing on GaAsSb-based materials. These intensive investigations indicate that the defects related to non-radiative recombination centers can be significant reduced by thermal treatment [4].

Carrier localization is a common phenomenon in semiconductors, which has been widely observed in alloys such as AlGaN [10–13], InGaN [14–16], InGaNP [17–19] and GaAsSb [20]. The behavior of carrier localization can be explained in terms of the excitons localized by potential fluctuation in semiconductors. From previous investigations, localized excitons can be identified easily through low temperature photoluminescence (PL) measurements. Besides, the trapped excitons were able to get sufficient thermal energy to de-trap at higher temperatures. Furthermore, carriers released from the localized states can contribute to the

[3] Authors to whom any correspondence should be addressed.

 © 2017 IOP Publishing Ltd Printed in the UK

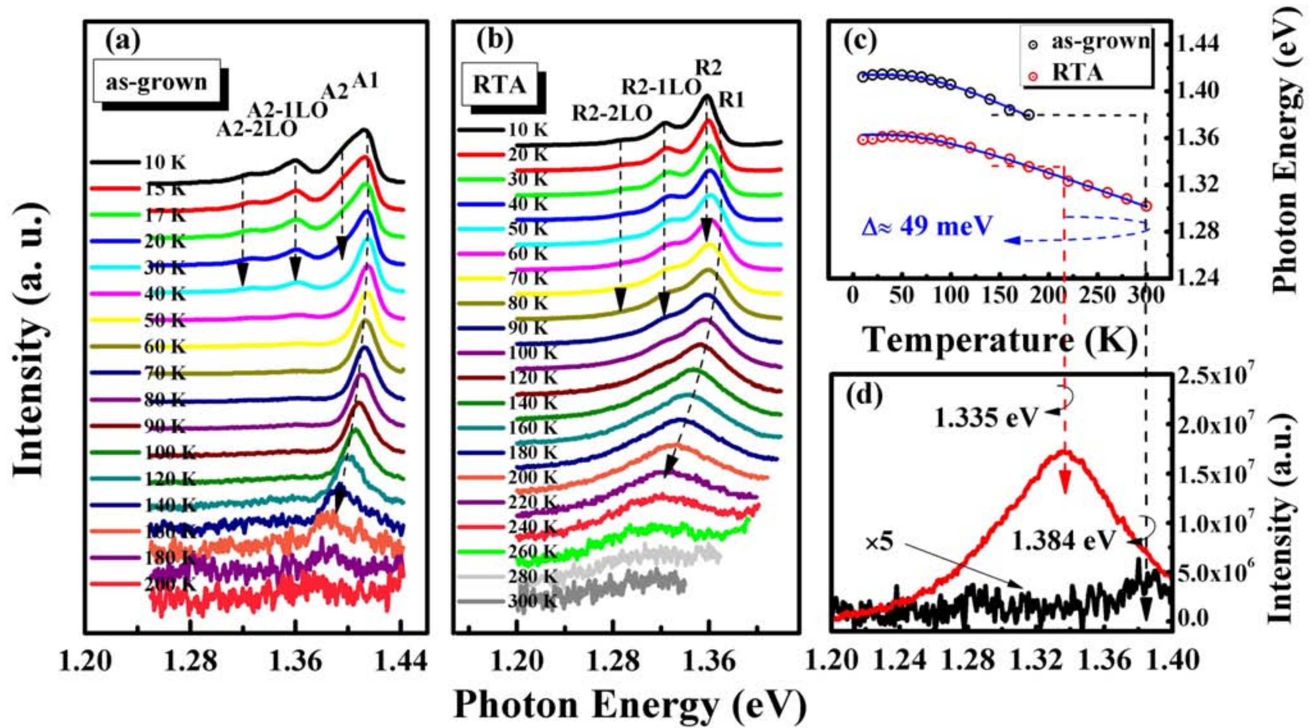

Figure 1. Temperature dependent PL spectra of (a) as-grown GaAsSb sample and (b) RTA treated GaAsSb alloy. (c) Temperature dependent peak positions of the as-grown and RTA sample. (d) PL spectra of as-grown and RTA sample at 180 K.

emission which can be maintained over a wide temperature range. However, many studies have shown that the quality of the material degrades under a higher degree of localization [21]. Therefore, researchers are committed to eliminating the localized states, for example, by using *in situ* or post thermal treatments [22, 23]. In our previous study [20], it was found that the localized degree displays a linear relationship with the Sb content. To eliminate the localized states, a rapid thermal annealing (RTA) process was used in later research [24]. It was found that a suitable annealing process could suppress defects or reduce localized states in GaAsSb alloys. However, carrier localized phenomenon was more serious when the samples were treated at a higher temperature.

In this letter, localized and delocalized states emissions of GaAsSb alloy are investigated. The GaAsSb sample is grown at a higher temperature (50 °C higher than the samples in references [20] and [24]) and with a lower Sb content of 5.5%. Interestingly, it is the first time that the near band edge emission from GaAsSb with multiple phonon replicas has been observed, and therefore it enables us to discuss the interaction between localized exciton and their longitudinal optical (LO) phonons. The experimental results showed the localized exciton and band edge related emission were enhanced after RTA treatment, and the band edge related emission could be maintained up to room temperature. Moreover, it is found that the exciton–LO phonon interaction depends strongly on the localized states. It can be concluded that the homogeneous distribution of Sb content can be promoted by optimal RTA conditions, which is useful for improving their device applications.

2. Experimental details

The GaAsSb sample was grown on a semi-insulating (001)-oriented GaAs substrate in a DCA P600 solid-source molecular beam epitaxy (MBE) system, which was equipped with As and Sb valved crackers for As_2 and Sb_2 beam species. The beam ratio was calibrated before growth and the cracker temperatures were 900 °C and 850 °C for As and Sb, respectively. The growth temperature of the GaAsSb was 650 °C, and the beam ratio of As/Sb was maintained at 7:1. The Sb content of the alloy was about 5.5%, which was deduced from the PL results. The structure of the GaAs substrate consists of an undoped GaAs buffer layer and a 350 nm GaAsSb layer.

A GaAsSb sample was treated by the RTA process after growth, with an annealing temperature of 700 °C for 30 s. The treatment of the annealing process was carried out under a nitrogen atmosphere. As-grown and treated GaAsSb samples were performed in a closed-cycle helium cryostat with CaF_2 windows for PL measurements. The PL spectra were recorded using a HORIBA iHR550 spectrometer, and detected with an InGaAs detector. A 655 nm CW semiconductor diode laser was used as the excitation source, and the power density could be adjusted from 0.1–240 mW cm^{-2}. The temperature of the PL measurement ranged from 10–300 K.

3. Results and discussion

Figure 1(a) presents the temperature dependent PL spectra of the as-grown GaAsSb sample. The emission spectra (at 10 K) was be divided into four parts, namely A1, A2, A2-1LO and A2-2LO, respectively. The peak positions fitted by Gaussian functions are located at 1.4122, 1.3916, 1.3596 and 1.3276 eV, respectively. The energy difference between A2, A2-1LO and A2-2LO is about 33 meV, which is close to the GaAs LO phonon energy of $E_{\mathrm{LO}} \approx 35$ meV [25]. Therefore, A2 could be indexed as a zero phonon line, while A2-1LO and A2-2LO are assigned to be its LO-phonon replicas. It is clear that the peak A1 redshifts with the increase in temperature, and the PL emission is almost quenched at about 200 K. The quenching of the emission was attributed to the thermal activated non-radiative recombinations from the defects in the as-grown GaAsSb sample. Moreover, the photon energy of A1 linearly decreases with temperature, which is in agreement with the band edge related emission. Because the peak A2 is located at a lower energy than A1, we speculate that this emission is related to the localized states in the as-grown GaAsSb sample.

Figure 1(b) shows the temperature dependent PL spectra of the RTA treated GaAsSb sample. The emission can be divided into four peaks at low temperatures, too. Similarly, the peaks of the RTA sample could be marked as R1, R2, R2-1LO and R2-2LO at 10 K, and the peak positions are located at 1.374, 1.359, 1.324 and 1.289 eV, respectively. The energy spacing between the R2, R2-1LO and R2-2LO peaks is about 35 meV. Thus R2-1LO and R2-2LO can be assigned to the LO phonon replicas of R2. It is clear that R2 dominates at low temperature. However, with the increase in temperature, the peak of R1 gradually reaches accretion and finally dominates the emission. In this case, R2 can be associated with the emission from the localized states because it has similar features as the as-grown GaAsSb sample. Furthermore, the PL emission could be observed up to 300 K. The enhanced PL emission after RTA treatment proved that non-radiative recombinations can be controlled by thermal treatment. It is noted that the main emission peak shows a redshift after RTA treatment. In order to analyze the evolvement of PL emission, the temperature dependent peak positions of the two samples are displayed at figure 1(c) (open circles). The change in the peak positions with temperature can be described by the band gap shrinkage model [26],

$$E_g = E_0 - \alpha T^2/(T + \beta), \tag{1}$$

where E_g is the band gap of the sample at 0 K, α is a constant and β is related to the Debye temperature. In figure 1(c), the solid lines exhibit the fitting curves based on equation (1). The results show that this model fits the experimental data over a wide range of temperatures. However, in the case of the RTA treated sample, the peak positions of the emission are deviated from the fitting curves, especially in the low temperature range. The photon energy of the experimental data shows an unusual trend as the temperature increases continuously. This phenomenon supports the existence of the emissions related to the localized states in the GaAsSb sample.

Figure 1(d) displays the PL spectra of the as-grown and RTA treated GaAsSb samples measured at 180 K. At this particular temperature, the peak position of the sample has redshifted to 49 meV after the RTA treatment. According to reference [27], the valence band can be modulated by incorporating Sb into GaAs, leading to a significant reduction in band gap [24]. It is noted that the PL emission of the as-grown GaAsSb sample almost disappears above 180 K. In contrast, the emission intensity of the RTA treated sample is much stronger. The enhanced emission of the RTA treated GaAsSb sample suggests an improvement in optical properties, which can be attributed to better Sb uniformity and the successful suppression of non-radiative recommendation centers.

To further explore the origin of the emission of GaAsSb sample, power-dependent PL measurements were performed. Figure 2(a) reveals the power-dependent PL spectra of the as-grown GaAsSb sample at 10 K. The power densities range from 1–240 mW cm^{-2}. The emissions are composed of A1 and A2 peaks. The peak A2 dominates the PL spectra when the power density is below 60 mW cm^{-2}. As the power density increases, the emission of A1 becomes stronger. Furthermore, the main peak exhibits a blueshift, which is due to the competition between A1 and A2. This blueshift can be ascribed to the saturation of the localized states which have a smaller density.

Figure 2(b) displays the PL integrated intensity of A1 and A2 under different power densities. According to the relationship between power density and integrated intensity, the experiment data can be fitted by as follows:

$$I = \eta I_0^{\alpha}, \tag{2}$$

where I_0 is the power density, η is the emission efficiency and the exponent α represents the radiative recombination mechanism of the emission [28]. The cycles are the experimental data of A1 and A2, while the solid lines show the fitting curves based on equation (2). The parameter α for A1 is about 2, which indicates that this emission is related to band edge transitions. For peak A2, the value of α is 1.21, which supports its excitonic recombination. This result proves that the A2 emission comes from localized exciton, which is also supported by the saturated effect discussed above.

Figure 3(a) shows the power-dependent PL spectra of the RTA treated GaAsSb sample at 10 K. It is clear that the peak position did not shift over the wide range of power densities. For peak R2, the value of parameter α is 0.96, which supports the excitonic transitions. Although the main emission is dominated by R2 under various power densities, the signal from peak R1 could still be observed when the power density was larger than 40 mW/cm^2. Moreover, the emission from R1 is easier to resolve at higher temperature. Figures 3(c) and (d) show the PL spectra and fitting curves of the RTA treated sample at 10 and 50 K, respectively. The fitting results represent that the percentage of R1 became larger at the higher temperature. And the reason can be attributed to the localized exciton dissociated to the free ones, and contributes

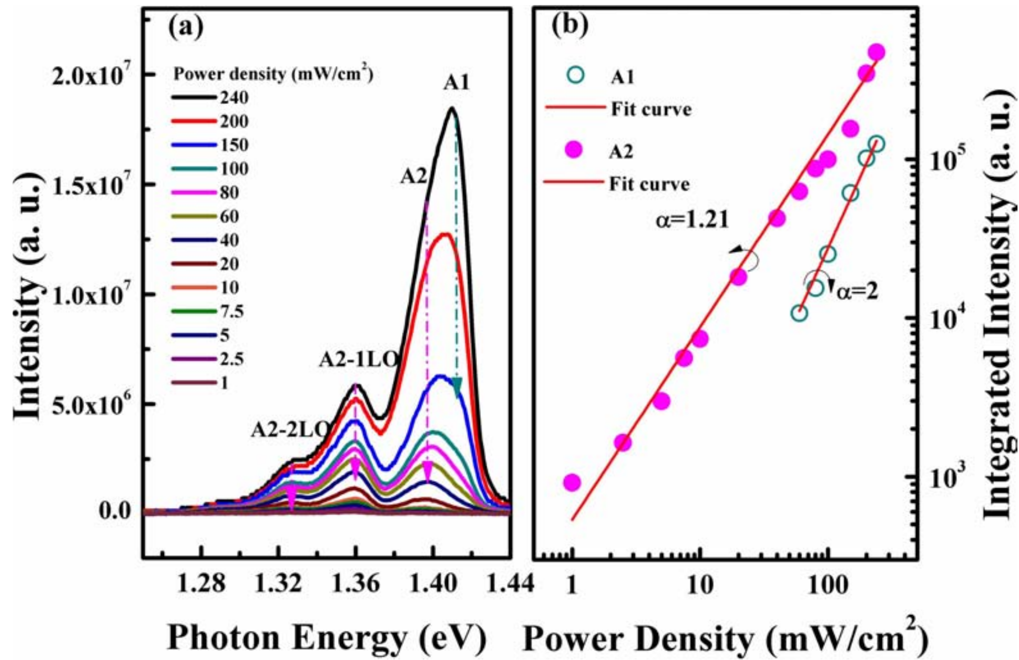

Figure 2. (a) Power-dependent PL spectra of as-grown GaAsSb sample at 10 K. (b) PL integrated intensity of peak A1 and A2 at various power densities, where the solid lines are fitting curves according to equation (2).

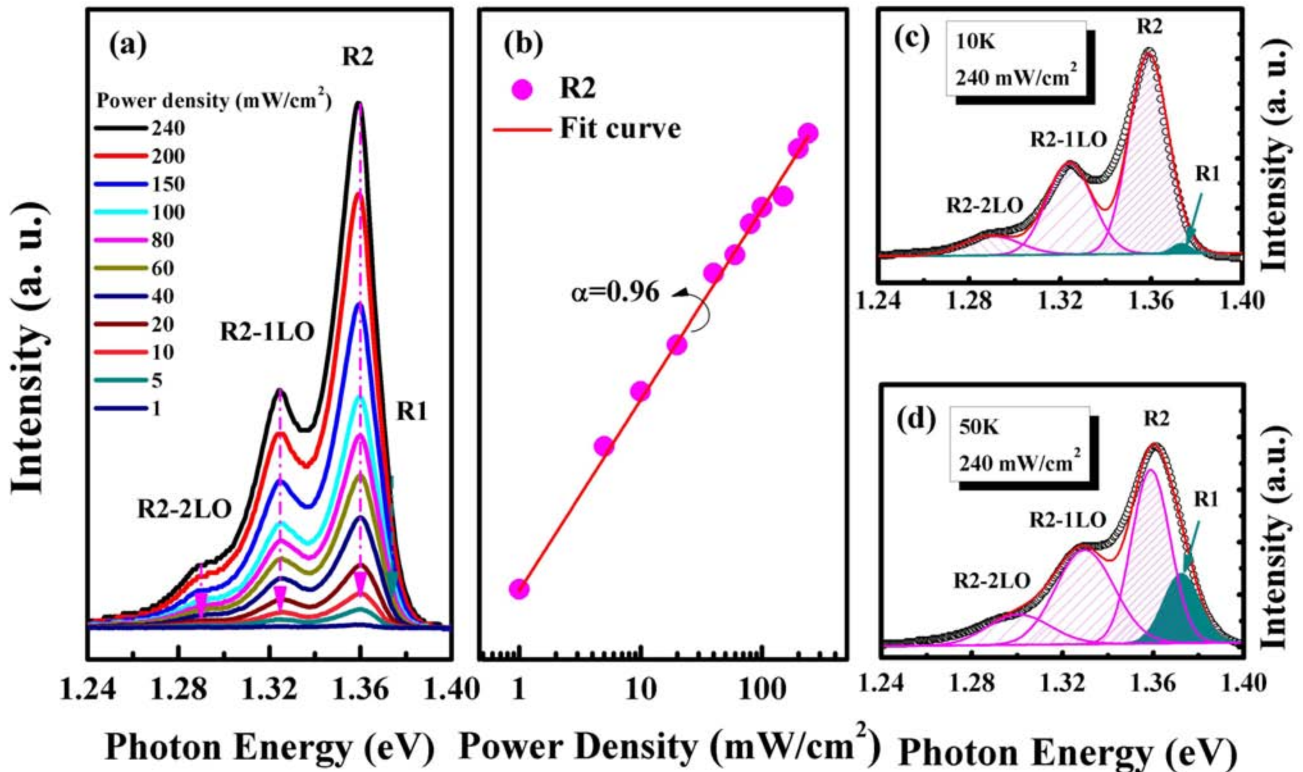

Figure 3. (a) Power-dependent PL spectra of RTA treated GaAsSb sample at 10 K. (b) PL integrated intensity of peak R2 at various power densities, where the solid lines are fitting curves according to equation (2). The PL spectra fitted by Gaussian functions under a power density of 240 mW cm^{-2}(c) at 10 K and (d) at 50 K.

to the band edge related emission. Meanwhile, a comparison displayed the presence of band edge emission R1 at various temperatures in the treated GaAsSb sample.

Figure 4 demonstrates the integrated intensities of peaks A2 and R2 as a function of the reciprocal of temperature. In the case of the as-grown GaAsSb sample, the localized emission A2 merges into A1 when the temperature is above

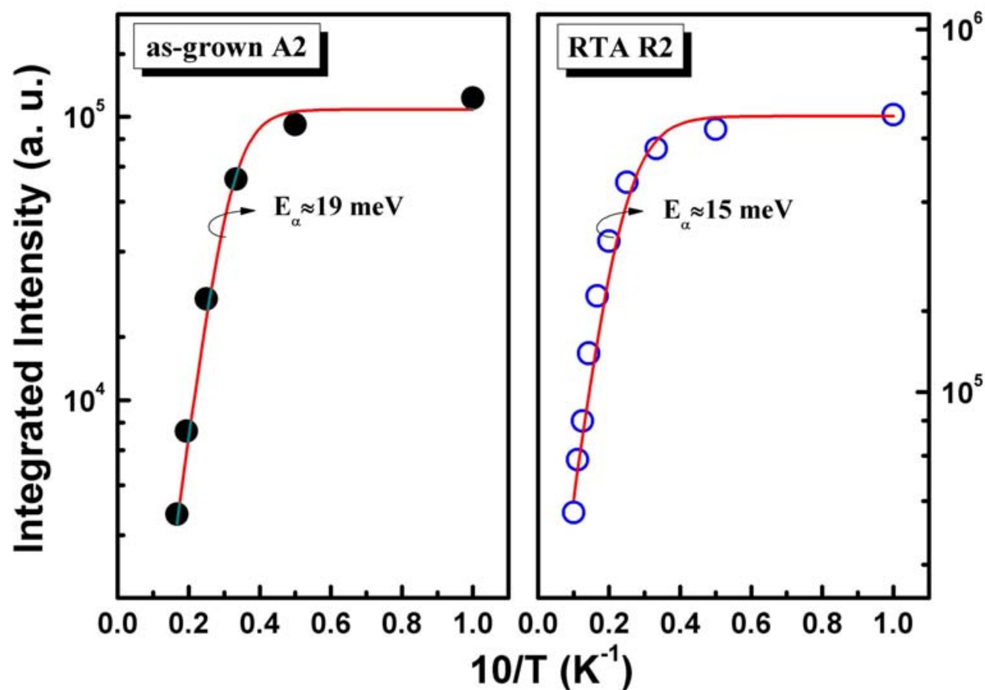

Figure 4. Integrated PL intensity of peak A2 (as-grown) and R2 (RTA treated) as a function of the reciprocal of temperature, respectively.

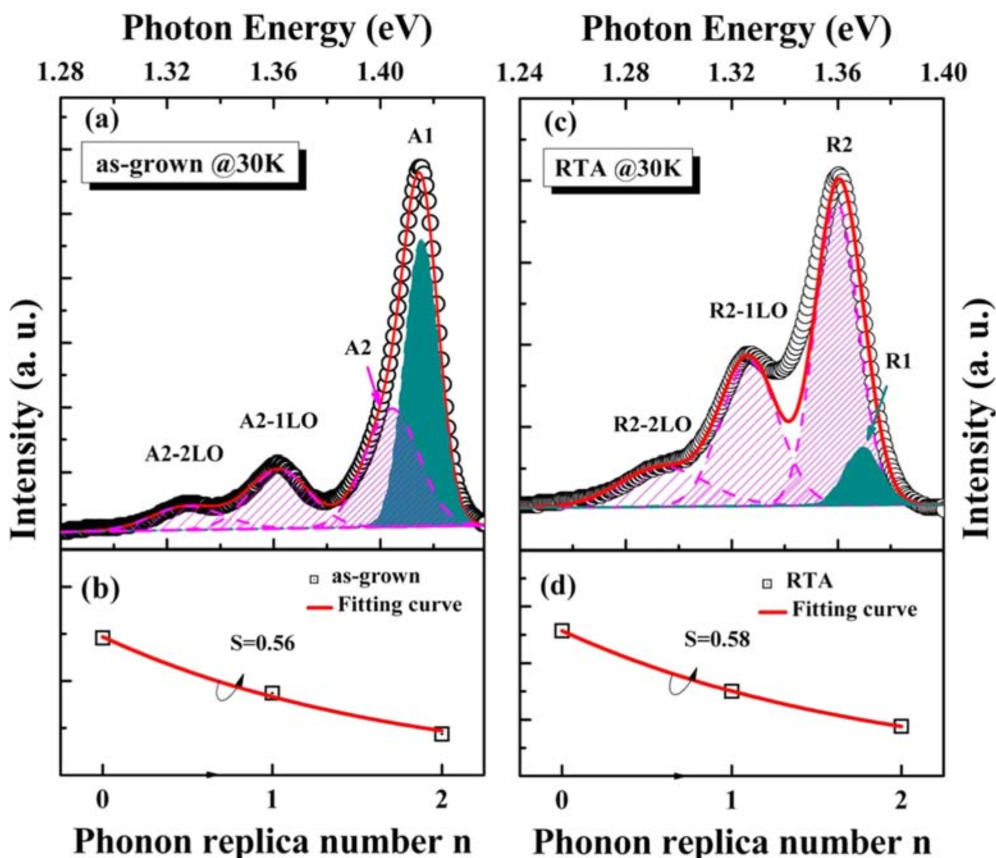

Figure 5. (a) PL spectra of as-grown GaAsSb sample and (b) RTA treated GaAsSb sample at 30 K (c) and (d) is the fitting based on equation (3) for the discussion of the localized exciton–LO-phonon coupling strength.

60 K. But for the RTA treated sample, the localized exciton R2 is quenched at 100 K. Therefore, the localized excitons are enhanced after RTA treatment. The trend of the temperature dependence quenching behavior of A2 and R2 can be described by an Arrhenius relationship [29]:

$$I = I_0[1 + a \times \exp(-E_a/k_B T)], \quad (3)$$

where E_a is the activation energy, k_B is the Boltzmann constant and a is a proportional constant. The value of E_a can be obtained from the fitting curve in figure 4. For A2 and R2, the obtained E_a values are 19 and 15 meV, respectively. These two values are approximately in agreement with the localization energy of the two samples, which is obtained from the energy difference between the free exciton and the localized exciton at low temperatures.

Finally, the emissions of the as-grown and RTA treated GaAsSb samples at 30 K are displayed in figure 5. The fitting curves are obtained based on Gaussian functions. According to the relationship between the zero phonon line (I_0) and its nth phonon replica (I_n), $I_n = I_0 S^n e^{-S}/n!$ [30–33], the Huang–Rhys factor (S) can be obtained. Based on figures 5(b) and (d), the deduced value of S is 0.56 and 0.58 for the as-grown and RTA treated samples, respectively. Apparently, S is slightly enhanced after RTA treatment. It is known that Huang–Rhys factor is related to the exciton–LO phonon coupling strength. For the as-grown sample, the existence of defects will lead to an imperfect lattice structure, and therefore the exciton–LO phonon coupling strength is interrupted. After RTA treatment, the removal of defects and dangling bonds will give rise to a better crystal structure, which will lead to a slightly bigger Huang–Rhys factor. This conclusion is in good agreement with the optical investigation described above.

Some Sb clusters form in the GaAsSb epilayer due to the competitive relation between the As_2 and Sb_2 species during the process of epitaxy. As a consequence, the localization states are generated and influence the emission. In the research carried out herein, the Sb content is only 5.5%, with a thickness of 350 nm. Therefore, the epilayer is under plastically relaxed, and the defects of threading dislocations could be controlled enormously. Based on the above results, it is reasonable to believe that the abnormal evolutions of PL spectra can be attributed to localized states, which are caused by the non-uniformity of the Sb content in the GaAsSb epilayer. On the other hand, non-radiative defects are also established in the alloy. Fortunately, RTA treatment can be used to mitigate the non-radiative defects, and the emission intensities are improved. It is worth noting that the interaction of localized exciton and LO phonon is discussed in this work. Besides, the Huang–Rhys factor (S) is slightly enlarged after RTA treatment, which strongly depends on the localized states.

4. Summary

In summary, the PL spectra of the GaAsSb samples are analyzed in detail over a wide temperature range. By evaluating the temperature and power-dependent emissions of the as-grown and RTA treated GaAsSb samples, the band edge and localized exciton related emissions are identified and discussed in detail. The PL emissions are almost quenched at 180 K for the as-grown GaAsSb, which can be attributed to thermal activated non-radiative recombinations. In contrast, for the RTA treated GaAsSb sample, the PL emissions are increased and can be maintained up to 300 K. Furthermore, the fitting results of the Huang–Rhys factor S indicate the interaction between the localized exciton and LO phonon is enhanced after RTA treatment, which is ascribed to the better crystal quality of the alloys. The results proved that non-radiative recombination defects, which were caused by non-uniform Sb content, can be decreased after suitable RTA treatment. Therefore, the emission properties of the GaAsSb materials can be improved.

Acknowledgments

This work is supported by the National Natural Science Foundation of China (11404161, 11574130, 61404009, 61474010, 61574022, 61504012, 61674021, 11404219, and 11674038), the Foundation of State Key Laboratory of High Power Semiconductor Lasers, the Developing Project of Science and Technology of Jilin Province (20160519007JH, 20160101255JC, 20160204074GX and 20170520117JH). The authors acknowledge the National 1000 plan for Young Talents and Shenzhen Science and Technology Innovation Committee (Projects Nos.:vJCYJ20150630162649956, JCYJ20150930160634263, JCYJ20160226192528793 and KQTD2015071710313656).

ORCID iDs

Rui Chen https://orcid.org/0000-0002-0445-7847

References

[1] Motyka M, Dyksik M, Ryczko K, Weih R, Dallner M, Höfling S, Kamp M, Sęk G and Misiewicz J 2016 Type-II quantum wells with tensile-strained GaAsSb layers for interband cascade lasers with tailored valence band mixing *Appl. Phys. Lett.* **108** 101905

[2] Ikyo A B, Marko I P, Hild K, Adams A R, Arafin S, Amann M and Cand Sweeney S J 2016 Temperature stable mid-infrared GaInAsSb/GaSb vertical cavity surface emitting lasers (VCSELs) *Sci. Rep.* **6** 619595

[3] Deutsch C *et al* 2010 Terahertz quantum cascade lasers based on type II InGaAs/GaAsSb/InP *Appl. Phys. Lett.* **97** 261110

[4] Wicaksono S, Yoon S F, Fan W J and Loke W K 2005 The effect of rapid thermal annealing on GaAsSbN quantum-well and GaAsSbN bulk lattice-matched to GaAs. Indium phosphide and related materials *Int. Conf. on. IEEE* 2005, 421–3

[5] Bremner S P, Ghosh K, Nataraj L, Cloutier S G and Honsberg C B 2010 Influence of Sb/As soak times on the

structural and optical properties of GaAsSb/GaAs interfaces *Thin Solid Films* **519** 64–8
[6] Hsu H P, Huang J K, Huang Y S, Lin Y T, Lin H H and Tiong K K 2010 Optical study of $GaAs_{1-x}Sb_x$ layers grown on GaAs substrates by gas-source molecular beam epitaxy *Mater. Chem. Phys.* **124** 558–62
[7] Nishino F, Takei T, Kato A, Jinbo Y and Uchitomi N 2005 Optical characterization of heavily Sn-Doped $GaAs_{1-x}Sb_x$ epilayers grown by molecular beam epitaxy on (001) GaAs substrates *Jpn. J. Appl. Phys.* **44** 705
[8] Qiu W, Wang X, Chen P, Li N and Lu W 2014 Optical spin polarization and Hanle effect in GaAsSb: temperature dependence *Appl. Phys. Lett.* **105** 082104
[9] Sigmund J, Sydlo C, Hartnagel H L, Benker N, Fuess H, Rutz F, Kleine-Ostmann T and Koch M 2005 Structure investigation of low-temperature-grown GaAsSb, a material for photoconductive terahertz antennas *Appl. Phys. Lett.* **87** 252103
[10] Bergman L, Dutta M, Stroscio M A, Komirenko S M, Nemanich R J, Eiting C J, Lambert D J H, Kwon H K and Dupuis R D 2000 Photoluminescence and recombination mechanisms in $GaN/Al_{0.2}Ga_{0.8}N$ superlattice *Appl. Phys. Lett.* **76** 1969
[11] Nepal N, Li J, Nakarmi M L, Lin J Y and Jiang H X 2006 Exciton localization in AlGaN alloys *Appl. Phys. Lett.* **88** 062103
[12] Merano M, Sonderegger S, Crottini A, Collin S, Pelucchi E, Renucci P and Deveaud B 2006 Time-resolved cathodoluminescence of InGaAs/AlGaAs tetrahedral pyramidal quantum structures *Appl. Phys. B: Lasers Opt.* **84** 343–50
[13] Liao Y, Thomidis C, Kao C K and Moustakas T D 2011 AlGaN based deep ultraviolet light emitting diodes with high internal quantum efficiency grown by molecular beam epitaxy *Appl. Phys. Lett.* **98** 081110
[14] Ko T S, Lu T C, Wang T C, Chen J R, Gao R C, Lo M H and Shen J L 2008 Optical study of a-plane InGaN/GaN multiple quantum wells with different well widths grown by metal-organic chemical vapor deposition *J. Appl. Phys.* **104** 093106
[15] Liu B, Smith R, Bai J, Gong Y and Wang T 2013 Great emission enhancement and excitonic recombination dynamics of InGaN/GaN nanorod structures *Appl. Phys. Lett.* **103** 101108
[16] Tsai C L and Wu W C 2014 Effects of asymmetric quantum wells on the structural and optical properties of InGaN-based light-emitting diodes *Materials* **7** 3758–71
[17] Hong Y G, Nishikawa A and Tu C W 2003 Effect of nitrogen on the optical and transport properties of $Ga_{0.48}In_{0.52}N_yP_{1-y}$ grown on GaAs (001) substrates *Appl. Phys. Lett.* **83** 5446–8
[18] Izadifard M, Bergman J P, Chen W M, Buyanova I A, Hong Y G and Tu C W 2006 Photoluminescence upconversion in Ga In NP/Ga As heterostructures grown by gas source molecular beam epitaxy *J. Appl. Phys.* **99** 073515
[19] Wang D, Jiao S, Zhao L, Liu T, Gao S, Li H, Wang J, Yu Q and Guo F 2012 Study of ultraviolet emission enhancement in $Al_xIn_yGa_{1-x-y}N$ quaternary alloy film *The J. Phys. Chem.* C **117** 543–8
[20] Gao X *et al* 2016 Investigation of localized states in GaAsSb epilayers grown by molecular beam epitaxy *Sci. Rep.* **6** 29112
[21] Erol A 2008 *Dilute III-V Nitride Semiconductors and Material Systems* 105 (Berlin Heidelberg: Springer) (https://doi.org/10.1007/978-3-540-74529-7)
[22] Kitatani T, Nakahara K, Kondow M, Uomi K and Tanaka T 2000 Mechanism analysis of improved GaInNAs optical properties through thermal annealing *J. Cryst. Growth* **209** 345
[23] Pan Z, Miyamoto T, Schlenker D, Sato S, Koyama F and Iga K 1998 Low temperature growth of GaInNAs/GaAs quantum wells by metalorganic chemical vapor deposition using tertiarybutylarsine *J. Appl. Phys.* **84** 6409
[24] Gao X, Wei Z, Fang X *et al* 2017 Effect of rapid thermal annealing on the optical properties of GaAsSb alloys[J]. Optical Materials *Opt. Mater. Express* **7** 1974
[25] Kash J A, Tsang J C and Hvam J M 1985 Subpicosecond time-resolved Raman spectroscopy of LO phonons in GaAs *Phys. Rev. Lett.* **54** 2151
[26] Varshni Y P 1967 Temperature dependence of the energy gap in semiconductors *Physica* **34** 149–54
[27] Reyes D F, Ulloa J M, Guzman A, Hierro A, Sales D L, Beanland R, Sanchez A M and González D 2015 Effect of annealing in the Sb and In distribution of type II GaAsSb-capped InAs quantum dots *Semicond. Sci. Technol.* **30** 114006
[28] Bergman L, Chen X B, Morrison J L, Huso J and Purdy A P 2004 Photoluminescence dynamics in ensembles of wide-band-gap nanocrystallites and powders *J. Appl. Phys.* **96** 675
[29] Schmidt T, Lischka K and Zulehner W 1992 Excitation-power dependence of the near-band-edge photoluminescence of semiconductors *Phys. Rev.* B **45** 8989
[30] Huang K and Rhys A 1950 Theory of light absorption and non-radiative transitions in F-centres *Proc. R. Soc. London, Ser. A* **204** 406
[31] Duke C B and Mahan G D 1965 Phonon-broadened impurity spectra: I. Density of states *Phys. Rev.* **139** A1965
[32] Heitz R, Mukhametzhanov I, Stier O, Madhukar A and Bimberg D 1999 Enhanced polar exciton-LO-phonon interaction in quantum dots *Phys. Rev. Lett.* **83** 4654
[33] Callsen G *et al* 2015 Analysis of the exciton-LO-phonon coupling in single wurtzite GaN quantum dots *Phys. Rev.* B **92** 235439